Otgonbaatar et al. BMC Medical Imaging (2025) 25:522
https://doi.org/10.1186/s12880-025-02082-5

BMC Medical Imaging

RESEARCH Open Access

Detection of intracranial hemorrhage using ultralow-dose brain computed tomography with deep learning reconstruction versus conventional-dose computed tomography

Chuluunbaatar Otgonbaatar[1,2], Hyunjung Kim[3], Pil-Hyun Jeon[3], Sang-Hyun Jeon[3], Sung-Jin Cha[3], Jae-Kyun Ryu[1], Hackjoon Shim[1,4], Sung Min Ko[3] and Jin Woo Kim[3*]

Abstract

Background This study aimed to evaluate the diagnostic performance, image quality, and radiation dose among ultralow-dose protocol with deep learning reconstruction (DLR), ultralow-dose computed tomography (CT) with iterative reconstruction (IR), and conventional-dose protocols for detecting intracranial hemorrhage.

Methods This retrospective study enrolled 93 patients (median age: 67 years; interquartile range [IQR]: 59–76 years; 61 males). A conventional-dose CT was obtained using 120 kVp, 123–188 mA and IR. Follow-up ultralow-dose CT was obtained using 120 kVp, 50 mA with IR and DLR. Qualitative assessments and quantitative assessments were conducted. The diagnostic performance for detecting intracranial hemorrhage was assessed.

Results An approximately 84.0% reduction in median volume CT dose index was found in the ultralow-dose CT protocol (5.6 mGy) compared with conventional-dose CT (35.02 mGy). Ultralow-dose CT with DLR significantly ($p < 0.001$) reduced image noise, improved signal-to-nosie ratio, and contrast-to-tnoise ratio compared with ultralow-dose CT with IR and conventional-dose CT. Ultralow-dose CT with DLR resulted in higher sensitivity (99.3% vs. 98.6%) and specificity (97.5% vs. 97.5%) for detecting intracranial hemorrhage than ultralow-dose CT with IR.

Conclusion Ultralow-dose CT with DLR is not inferior to conventional-dose CT in terms of image quality and diagnostic performance for the detection of intracranial hemorrhage, while achieving an approximate 87.7% reduction in radiation dose.

Keywords Ultralow-dose CT, Haemorrhage, Brain, Deep learning reconstruction

*Correspondence:
Jin Woo Kim
sunny-cocktail@hanmail.net
[1]Medical Imaging AI Research Center, Canon Medical Systems Korea, Seoul, Republic of Korea
[2]Department of Radiology, School of Medicine, Mongolian National University of Medical Sciences, Ulaanbaatar, Mongolia
[3]Department of Radiology, Wonju Severance Christian Hospital, Wonju College of Medicine, Yonsei University of Korea, 20 Ilsan-ro, Wonju, Gangwon 26426, Republic of Korea
[4]ConnectAI Research Center, Yonsei University College of Medicine, Seoul, Republic of Korea

Introduction

Noncontrast computed tomography (CT) is a primary imaging modality used to rule out various acute conditions, particularly trauma, brain intracranial hemorrhage, or acute neurologic deficits in emergency settings [1]. Repeated imaging is often required for monitoring hemorrhagic progression, post-operative evaluation, or assessment of treatment response, particularly in patients with extended hospital stays. This is especially relevant in younger patients, for whom minimizing cumulative radiation exposure is of critical importance. Concerns persist regarding decreasing the radiation dose as low as reasonably achievable, while maintaining sufficient image quality for accurate diagnosis. Accordingly, the implementation of reduced-dose CT protocols is clinically essential to mitigate the long-term risks associated with ionizing radiation. Several studies have revealed that high radiation doses are associated with an increased risk of lenticular changes, cortical cataracts, cancer, DNA effects, and chromosome aberrations [2–5].

The radiation dose is directly proportional to tube voltage and tube current [6]. The use of a low-dose radiation protocol reduces the radiation dose in brain CT angiography. However, it still demonstrates higher image noise and lower signal-to-noise ratio (SNR) in noncontrast brain CT because of skull thickness [7]. Image reconstruction is the best way to optimize the tradeoff between radiation dose and image noise among different approaches. Dieckmeyer et al. revealed a dose reduction ranging from 18% to 66% in noncontrast brain CT (volume CT dose index of 10.8–41.0 mGy) using a combination of reduced-dose protocol and iterative reconstruction (IR) method while maintaining image quality for evaluating intracranial hemorrhage in their systematic review [1]. Unfortunately, noncontrast brain CT protocols failed to detect intracranial results in patients with acute neurologic deficit, even with the combination of a reduced-dose protocol (volume CT dose index of 7.6 mGy) with IR [8].

Conversely, advances in technology, specifically commercially available deep learning image reconstruction (DLR) algorithms including Advanced Intelligent Clear-IQ Engine (Canon Medical Systems), TrueFidelity (GE Healthcare), and Precise image (Philips Healthcare), have offered the potential to enhance image quality by reducing image noise, minimizing artifacts, and achieving higher SNR through a deep convolutional neural network compared with commonly used IR [9–13]. However, to date, no study has focused on the application of ultralow-dose protocol with DLR for evaluating intracranial hemorrhage in comparison with conventional-dose protocol with IR. Therefore, we aimed to evaluate the diagnostic performance, image quality, and radiation dose among ultralow-dose protocol with DLR, ultralow-dose CT with IR, and conventional-dose protocols for detecting intracranial hemorrhage.

Materials and methods

This retrospective study was approved by the Institutional Review Board of Wonju Severance Christian Hospital (IRB number: CR323171). The requirement for informed consent was waived because of the retrospective study design. The study was performed in accordance with relevant guidelines and regulations, including the Declaration of Helsinki. This study included patients who were referred for unenhanced brain CT examinations between October 2023 and December 2023. All patients underwent follow-up noncontrast CT with an ultralow-dose setting after the initial conventional-dose CT. Patients were excluded if a) images exhibited motion artifacts ($n = 5$) and b) > 5 days between conventional-dose CT and ultralow-dose CT follow-up ($n = 10$).

Image acquisition

All patients were scanned with a 320-multidetector row CT (Aquilion ONE PRISM Edition, Canon Medical Systems Corporation, Otawara-si, Japan) and 192-multidetector row CT (SOMATOM Force, Siemens Healthcare, Forchheim, Germany). The conventional-dose CT images were acquired at a tube voltage of 120 kVp, field of view of 200 mm, slice thickness of 0.6 mm, rotation time of 1 s, image reconstruction of advanced modeled IR - HR44 kernel, and a reconstruced slice thickness of 5 mm. Automatic exposure control (^{SURE}Exposure; Canon Medical Systems Corporation) was applied for the tube current (123–188 mA). The follow- up ultralow-dose setting [8] was performed at a tube voltage of 120 kVp, tube current of 50 mA, field of view of 190 mm, slice thickness of 0.5 mm, rotation time of 1 s, image reconstruction of deep learning reconstruction method–brain standard option (DLR; Advanced intelligent clear-IQ engine, AiCE, Canon Medical Systems Corporation) and hybrid IR – FC26 kernel (Adaptive Iterative Dose Reduction 3-D, AIDR-3D, Canon Medical Systems Corporation), and a reconstructed slice thickness with 5 mm. Table 1 summarizes the scanning protocol.

Dose calculation

Volume CT dose index ($CTDI_{vol}$) and dose-length product (DLP) for each patient were recorded. The effective radiation dose was calculated by multiplying the DLP by a conversion coefficient of 0.0023 for the head [14].

Qualitative and quantitative image quality analysis

The image noise was calculated as the standard deviation (SD) of a 30 mm^2 spherical region of interest (ROI) in the lateral ventricle cerebrospinal fluid (CSF). Spherical ROIs measuring 20 mm^2 were placed in the white matter

Table 1 Scanning protocol among conventional and ultralow-dose CT

	Conventional CT	Ultralow-dose with DLR	Ultralow-dose with IR
CT scanner	SOMATOM Force	Aquilion ONE PRISM	Aquilion ONE PRISM
Tube voltage (kilovoltage)	120	120	120
Tube current (milli-ampere)	123–188	50	50
Reconstructed slice thickness (mm)	5	5	5
Scan length (mm)	180	160	160
Rotation time (sec)	1	1	1
Field of view (mm)	200	190	190
Image reconstruction	Advanced modeled iterative reconstruction	Deep learning reconstruction	Hybrid iterative reconstruction
DLP (mGy • cm)*	35.02 (33.09–37.36)	5.6	5.6
$CTDI_{vol}$ (mGy)*	733.2 (699.9–814.4)	90.1	90.1

*Data are presented as medians (interquartile ranges). Volume CT dose index ($CTDI_{vol}$), dose-length product (DLP)

of the internal capsule and gray matter of the thalamus at the basal ganglia level to assess white and gray matter. The SNR for white and gray matter was calculated as the CT attenuation number divided by SD. The contrast-to-noise ratio (CNR) for white and gray matter was calculated as the difference in the mean CT number between gray matter (GM) and white matter (WM), divided by the square root of the sum of their variances [15].

Two board-certified radiologists with 10 and 6 years of experience in neuroradiology, respectively, independently evaluated the image quality. Each observer was blinded to the conventional-dose CT protocol, ultralow-dose CT with DLR, and ultralow-dose CT with IR. They were randomly rated on a five-point scale as follows: 5, excellent image quality with very low image noise, excellent differentiation between white and gray matter, and no artifact; 4, good image quality with low image noise, good differentiation between white and gray matter, and mild artifact; 3, moderate image quality with average image noise, moderate differentiation between white and gray matter, and moderate artifact; 2, fair image quality with above average noise, blurry between white and gray matter differentiation, and severe artifact; 1, poor image quality with unacceptable image noise, very blurry between white and gray matter differentiation, and very severe artifact [16].

Table 2 Patient demographic characteristics

	All cases (*n* = 91)
Age, years (IQR)	67 (59–71)
Male sex, n (%)	61 (67.0%)
Medical history	
Diabetes, n (%)	28 (30.1%)
Hypertension, n (%)	41 (44.1%)
Hyperlipidemia, n (%)	9 (9.7%)
Current smokers, n (%)	15 (16.1%)

Data are presented as medians (interquartile ranges). Otherwise, data are number of patients with % in parentheses. IQR: interquartile range

Statistical analysis

The Kolmogorov–Smirnov and Shapiro–Wilk tests were used to assess data normality. Continuous variables are reported as medians and interquartile ranges (IQR). Image noise, SNR, CNR, and qualitative image analysis scores were compared among ultralow-dose CT with DLR, ultralow-dose CT with IR, and conventional-dose CT using the Friedman test. Dunn's post-hoc test was performed for multiple comparisons. DLP, $CTDI_{vol}$, and effective doses were compared between ultralow-dose CT and conventional-dose CT using the Mann–Whitney test. The interclass correlation coefficient (ICC) was used for the observer agreement, where ICC values of < 0.21, 0.21–0.40, 0.41–0.60, 0.61–0.80, and >0.8 indicated poor, fair, moderate, strong, and near complete agreement, respectively [17]. Conventional-dose CT was used as the reference standard. The sensitivity, specificity, positive predictive value, and negative predictive value between conventional-dose CT, ultralow-dose CT with IR, and ultralow-dose CT with DLR were assessed by the McNemar test for each radiologist and generalized for the pooled radiologists. A *p*-value of < 0.05 was considered statistically significant. Statistical analysis was performed using Statistical Package for the Social Sciences statistical software version 25.0 (IBM, Armonk, NY, USA).

Results

Patients

This study included 93 patients (median age: 67 years; IQR: 59–76 years; 61 males). Table 2 summarizes patient demographic characteristics. The distribution of intracranial hemorrhage subtypes was as follows: intraparenchymal hemorrhage in 43 patients, subarachnoid hemorrhage in 28, subdural hematoma in 8, epidural hematoma in 4, and intraventricular hemorrhage in 4 patients.

Radiation dose

Ultralow-dose CT (90.1 mGy • cm) resulted in an approximately 87.7% reduction in median DLP compared with conventional-dose CT (733.2 mGy • cm; IQR: 669.9–814.4). An approximately 84.0% reduction in median $CTDI_{vol}$ was found in the ultralow-dose CT protocol (5.6 mGy) compared with conventional-dose CT (35.02 mGy; IQR: 33.09–37.36). The effective dose in mSv was 1.69 (IQR: 1.54–1.87) for ultra-dose CT and 0.21 for ultralow-dose CT.

Qualitative and quantitative image quality

Ultralow-dose CT with DLR (2.11; IQR: 1.74–2.59, 95% CI: 2.09–2.36) demonstrated approximately 2.66 and 1.97 times less image noise in CSF than ultralow-dose CT with IR (5.62; IQR: 4.92–6.32, 95% CI: 5.49–5.91) and conventional-dose CT (4.15; IQR: 3.81–4.62, 95% CI: 4.01–4.29) ($p < 0.001$). The post-hoc Dunn's test revealed a significant difference in the pairwise comparison between ultralow-dose CT with DLR, ultralow-dose CT with IR, and conventional-dose protocols ($p < 0.001$). Additionally, image noise in white matter (WM) and gray matter (GM) was significantly ($p < 0.001$) lower in ultralow-dose CT with DLR than in ultralow-dose CT with IR and conventional-dose CT (Fig. 1). Table 3 presents the results of CT attenuation, SNR, and CNR in WM and GM among ultralow-dose CT with DLR, ultralow-dose with IR, and conventional-dose CT. The median CT attenuation of WM and GM caused significantly higher CT attenuation for ultralow-dose CT with DLR compared with conventional-dose CT and ultralow-dose CT with IR ($p < 0.001$). SNR in WM and GM was significantly ($p < 0.001$) improved in ultralow-dose CT with DLR (WM = 12.8; IQR: 10.2–17.2 and GM = 21.2; IQR: 16.0–27.0) compared with ultralow-dose CT with IR (WM = 5.92; IQR: 4.98–7.00 and GM = 7.65; IQR: 6.80–8.76) and conventional-dose CT (WM = 7.60; IQR: 6.88–8.84 and GM = 9.13; IQR: 8.21–10.7). The post-hoc Dunn's test revealed a significant difference between each of the different images ($p < 0.001$). Additionally, a statistically significant difference ($p < 0.001$) in the CNR was found between different images.

Figure 2 summarizes the qualitative image analysis. The overall image quality ($p = 0.05$), image noise ($p = 0.07$), differentiation of gray and white matter ($p = 0.99$), and

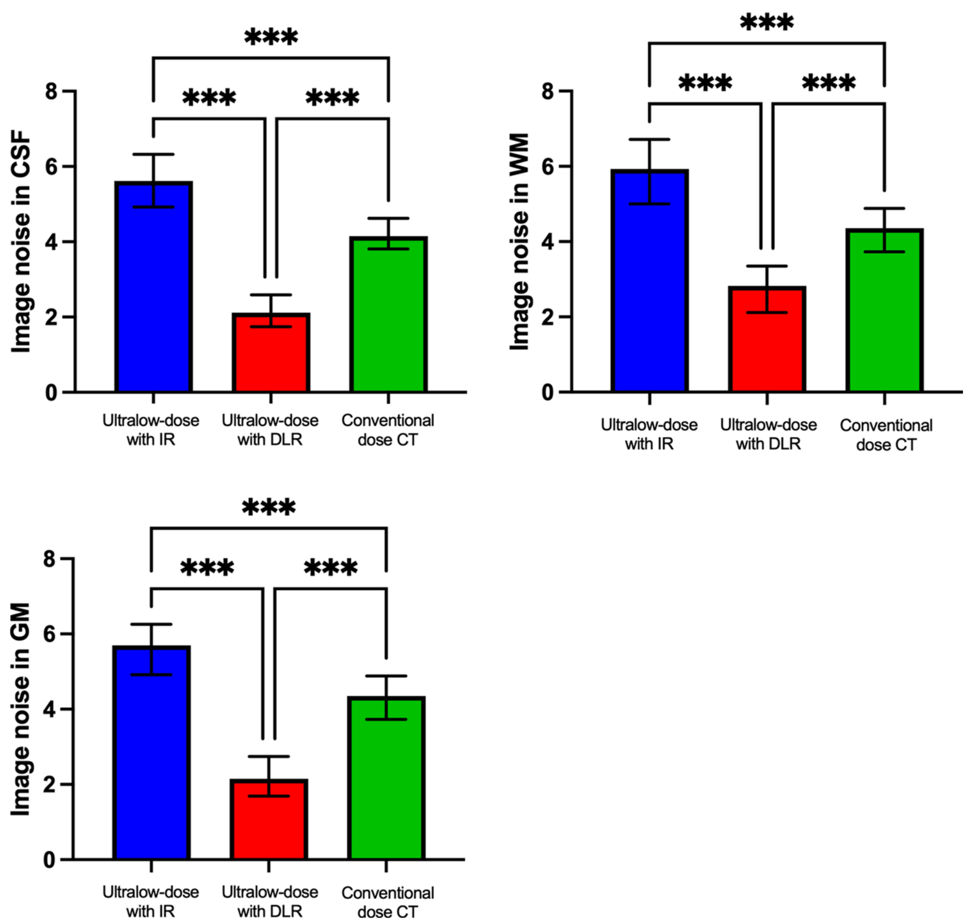

Fig. 1 Results of image noise among different image protocols and image reconstructions. Ultralow-dose CT with deep learning reconstruction (DLR) significantly lower image noise in cerebrospinal fluid (CSF), white matter (WM), and gray matter (GM) than ultralow-dose CT with iterative reconstruction (IR) and conventional-dose CT ($p < 0.001$). The post-hoc Dunn's test showed a significant difference in the pairwise comparison between ultralow-dose CT with DLR, ultralow-dose CT with IR, and conventional-dose protocols ($p < 0.001$). CSF: cerebrospinal fluid, WM: white matter, GM: gray matter, DLR: deep learning reconstruction, IR: iterative reconstruction. *** indicates $p < 0.001$

Table 3 Results of SNR and CNR among ultralow-dose CT with DLR, ultralow-dose CT with IR, and conventional-dose CT

	Ultralow-dose CT with IR (A)	Ultralow-dose CT with DLR (B)	Conventional-dose CT (C)	*P*-value (A vs. B vs. C)	A vs. B	A vs. C	B vs. C
CT attenuation in WM	35.5 (33.3–37.5) [34.7–36.1]	36.1 (33.8–38.1) [35.6–37.0]	32.9 (31.1–34.5) [32.4–33.7]	< 0.001	< 0.001	< 0.001	< 0.001
CT attenuation in GM	43.7 (42.1–45.3) [42.4–43.7]	46.1 (44.6–47.1) [44.9–46.0]	40.7 (39.7–42.1) [39.8–41.1]	< 0.001	< 0.001	< 0.001	< 0.001
SNR in WM	5.92 (4.98–7.00) [5.90–6.52]	12.8 (10.2–17.2) [12.9–15.3]	7.60 (6.88–8.84) [7.76–8.92]	< 0.001	< 0.001	< 0.001	< 0.001
SNR in GM	7.65 (6.80–8.76) [7.54–8.22]	21.2 (16.0–27.0) [20.2–23.7]	9.13 (8.21–10.7) [9.35–11.1]	< 0.001	< 0.001	< 0.001	< 0.001
CNR	2.51 (1.93–3.03) [2.33–2.61]	4.30 (3.63–5.46) [4.16–4.72]	2.67 (2.13–3.25) [2.62–3.06]	< 0.001	< 0.001	0.02	< 0.001

Data are reported as medians (interquartile ranges), [95% confidence intervals]. WM: white matter, GM: gray matter, SNR: signal-to-noise ratio, CNR: contrast-to-noise ratio, DLR: deep learning reconstruction, IR: iterative reconstruction

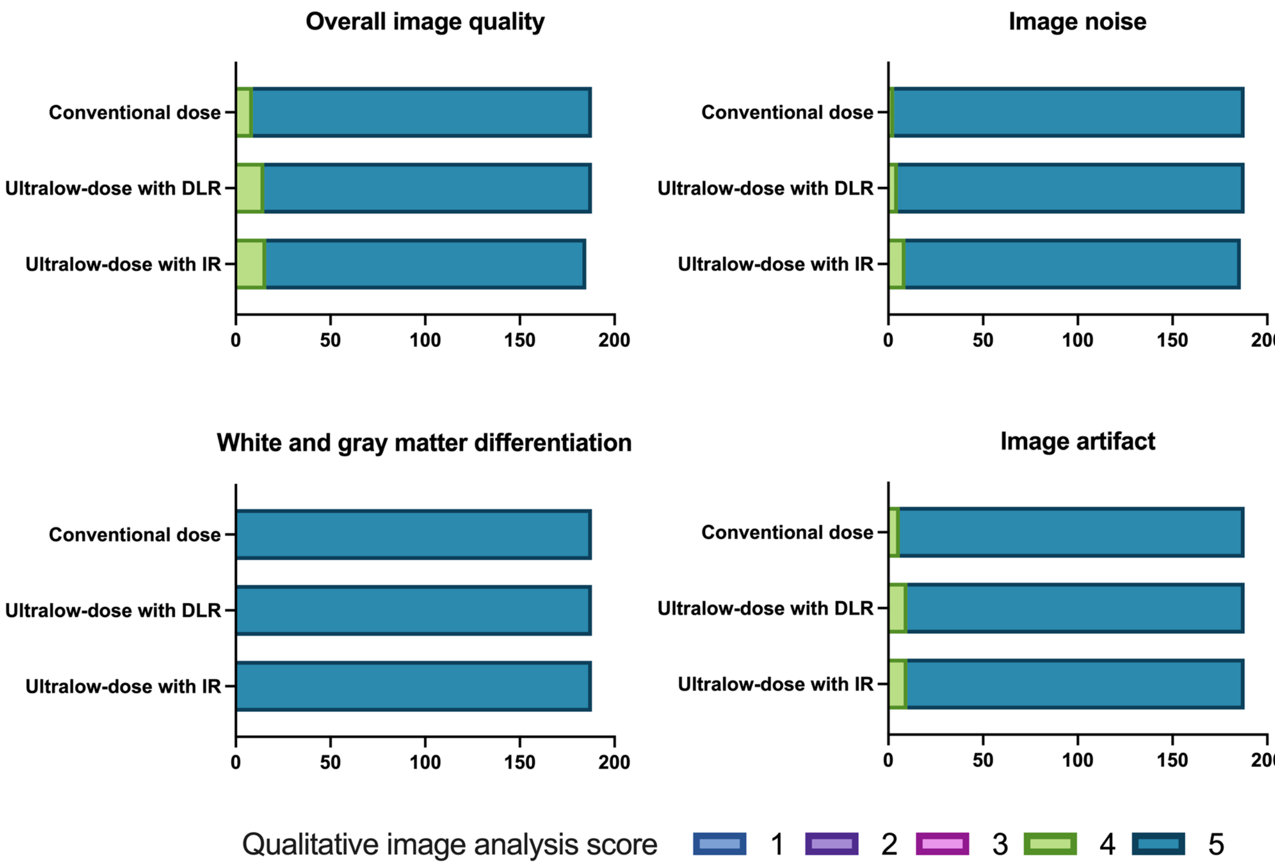

Fig. 2 Results of qualitative image analysis. Overall image quality ($p = 0.05$), image noise ($p = 0.07$), differentiation of gray and white matter ($p = 0.99$), and artifact ($p = 0.39$) demonstrated no significant differences between ultralow-dose with iterative reconstruction (IR), ultralow-dose with deep learning reconstruction (DLR), and conventional-dose CT. The interobserver agreement resulted in moderate (ICC = 0.463; 95% CI: 0.396–0.522) for qualitative image analysis. DLR: deep learning reconstruction, IR: iterative reconstruction

artifact ($p = 0.39$) demonstrated no significant differences between ultralow-dose with IR, ultralow-dose with DLR, and conventional-dose CT. The interobserver agreement resulted in moderate (ICC = 0.463; 95% confidence interval [CI]: 0.396–0.522) for qualitative image analysis between the two observers.

The pooled radiologists resulted in higher sensitivity (99.3% [145/146] vs. 98.6% [144/146]) and specificity (97.5% [39/40] vs. 97.5% [39/40]) for ultralow-dose CT with DLR in detecting intracranial hemorrhage compared with ultralow-dose CT with IR (Table 4). Figures 3 and 4 illustrate the representative cases.

Table 4 Hemorrhage detection with ultralow-dose protocols compared with conventional dose CT

		Sensitivity (%)	Specificity (%)	PPV (%)	NPV (%)
Reader 1	Ultralow-dose with IR	97.3 (90.7–99.5)	100 (82.2–100)	100 (94.9–100)	90.5 (71.1–98.3)
	Ultralow-dose with DLR	98.6 (92.7–99.9)	100 (83.2–100)	100 (95.0–100)	95 (76.4–99.7)
Reader 2	Ultralow-dose with IR	100 (94.9–100)	95.2 (77.3–99.8)	98.6 (92.6–99.9)	100 (83.9–100)
	Ultralow-dose with DLR	100 (94.9–100)	95.2 (77.3–99.8)	98.6 (92.6–99.9)	100 (83.9–100)
Pooled readers	Ultralow-dose with IR	98.6 (95.1–99.8)	97.5 (87.1–99.9)	99.3 (96.2–100)	95.1 (83.9–99.1)
	Ultralow-dose with DLR	99.3 (96.2–100)	97.5 (87.1–99.9)	99.3 (96.2–100)	97.5 (87.1–99.9)

Data are reported as (95% confidence intervals). DLR: deep learning reconstruction, IR: iterative reconstruction, PPV: positive predictive value, NPV: negative predictive value

Discussion

The present study investigated the value of ultralow-dose CT with DLR for the assessment of image quality and the evaluation of intracranial hemorrhage compared with ultralow-dose CT with IR and conventional-dose CT. Image quality was significantly improved in terms of image noise, SNR, and CNR, and higher diagnostic performance was observed with ultralow-dose CT with DLR than with ultralow-dose CT with IR.

Among commercially available DLRs released by vendors, TrueFidelity (GE Healthcare) and Precise (Philips Healthcare) DLRs were trained using images reconstructed with traditional filtered-back projection as the reference standard, whereas AiCE (Canon Medical Systems) was trained using routine-dose full mobel based-iterative reconstruction images as the ground truth to effectively differentiate between signals and noise [18, 19]. CT attenuation was significantly higher in ultralow-dose CT with DLR compared with other images; however, these differences were not clinically relevant, consistent with previous studies [20, 21]. Ultralow-dose CT protocols with deep learning denoising software have been successfully implemented in noncontrast CT for evaluating craniosynostosis in pediatric patients [22]. Their study demonstrated preserved diagnostic performance for craniosynostosis at an ultralow-radiation dose protocol (effective dose = 0.05 mSv) compared with routine-dose CT (effective dose = 1.15 mSv), but they revealed lower image quality with higher image noise for ultralow-dose CT despite using deep learning denoising software. Contrary to the results of the previous study, ultralow-dose CT with DLR in the present study revealed markedly higher image quality than ultralow-dose CT with IR and conventional-dose CT protocols. The use of DLR in ultralow-dose CT significantly reduced image noise by 2.66 and 1.97 times and improved SNR and CNR by approximately >2 times compared with ultralow-dose CT with IR and conventional-dose CT, respectively. The reduction of image noise, improvement of SNR and CNR not only helps to detect subtle findings including perlisional edema and small sized hemorrhage, but also increase the anatomical delination. The superior noise suppression and contrast enhancement achieved with DLR facilitate clearer anatomical delineation, improving the visibility of fine structures such as the margins of intracranial hemorrhage, perilesional edema, or small-volume bleeds—findings that may otherwise be missed in high-noise environments. This is particularly important in noncontrast brain CT, where the detection of hemorrhagic lesions relies heavily on gray–white matter differentiation. Conversely, ultralow-dose CT with IR caused higher image noise, lower SNR, and decreased CNR than conventional-dose CT. Therefore, these results emphasize the strength of DLR even in the ultralow-dose CT protocol compared with IR.

Sufficient radiation dose is required for interpreting changes in the brain parenchyma [9, 23]. Fletcher et al. revealed that the low-dose CT protocol (15.2 mGy) with IR caused preserved diagnostic performance for assessing acute neurologic deficit against routine-dose CT protocol but failed to detect intracranial hemorrhage at 7.6 mGy [8]. To our knowledge, this is the first study to investigate the image quality and detection of intracranial hemorrhage in an ultralow-dose CT protocol (5.6 mGy) with DLR against a conventional-dose CT protocol in the same patients. Additionally, ultralow-dose CT with DLR caused higher sensitivity (99.3% vs. 98.6%) and specificity (97.5% vs. 97.5%) for detecting intracranial hemorrhage than ultralow-dose CT with IR.

Some authors revealed that a higher incidence of cancer is associated with radiation exposure from CT, particularly in pediatric patients [24–26]. DNA double-strand breaks are considered the most harmful consequence of radiation exposure, leading to carcinogenesis [27, 28]. The study by Sakane et al. demonstrated a significant association between DNA double-strand break and

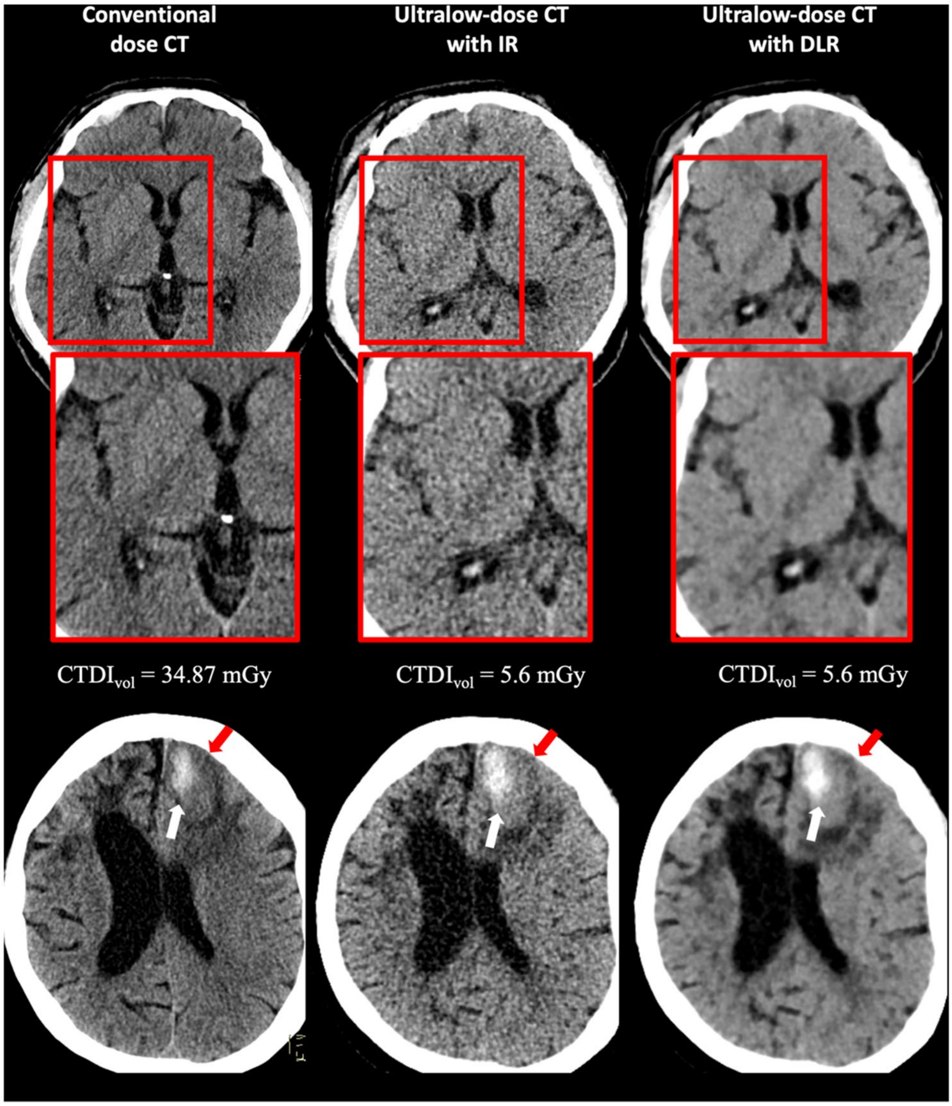

Fig. 3 Representative case of axial CT image with ultralow-dose CT. Axial CT images of a conventional-dose CT, ultralow-dose CT with iterative reconstruction (IR), and ultralow-dose CT with deep learning reconstruction (DLR). The volume CT dose index (CTDI$_{vol}$) was markedly lower with ultralow-dose CT (5.6 mGy) than with conventional-dose CT (34.87 mGy). Additionally, ultralow-dose CT with DLR revealed significantly lower image noise and better depiction of deep gray matter compared with ultralow-dose CT with IR and conventional dose CT. Perilesional edema (red arrow) and hemorrhagic margins (white arrows) were more clearly visualized with DLR compared to IR. Volume CT dose index: CTDI$_{vol}$, DLR: deep learning reconstruction, IR: iterative reconstruction

standard-dose CT protocol, whereas no remarkable association was observed between DNA double-strand break and low-dose CT [29]. Unfortunately, cumulative effective radiation doses from repeat or multiple CTs could increase the risk of cancer [30]. However, radiation exposure from CT should be minimized using optimal image parameters without compromising image quality and diagnostic performance. Our results strongly confirm the use of DLR in the ultralow-dose CT protocol. In general, low-dose CT is achieved by decreasing the tube voltage, lowering the tube current, reducing the gantry rotation time, and increasing the pitch [6]. Decreasing the tube voltage results in a lower radiation dose, but this method has disadvantages, particularly lower X-ray penetration in the skull. However, reducing the gantry rotation time and increasing the pitch allows a decrease in radiation exposure, thereby potentially affecting the spatial resolution. Moreover, lower radiation exposure with lower tube current causes higher image noise. Therefore, the most optimal approach to achieving an ultralow-radiation dose protocol is to decrease the tube current and use DLR. The use of a tube voltage of 120 kVp and a fixed tube current of 50 mA with DLR reduced the DLP by 87.7% and CTDI$_{vol}$ by 84.0% compared with the conventional-dose CT protocol, without decreasing the image quality and diagnostic performance.

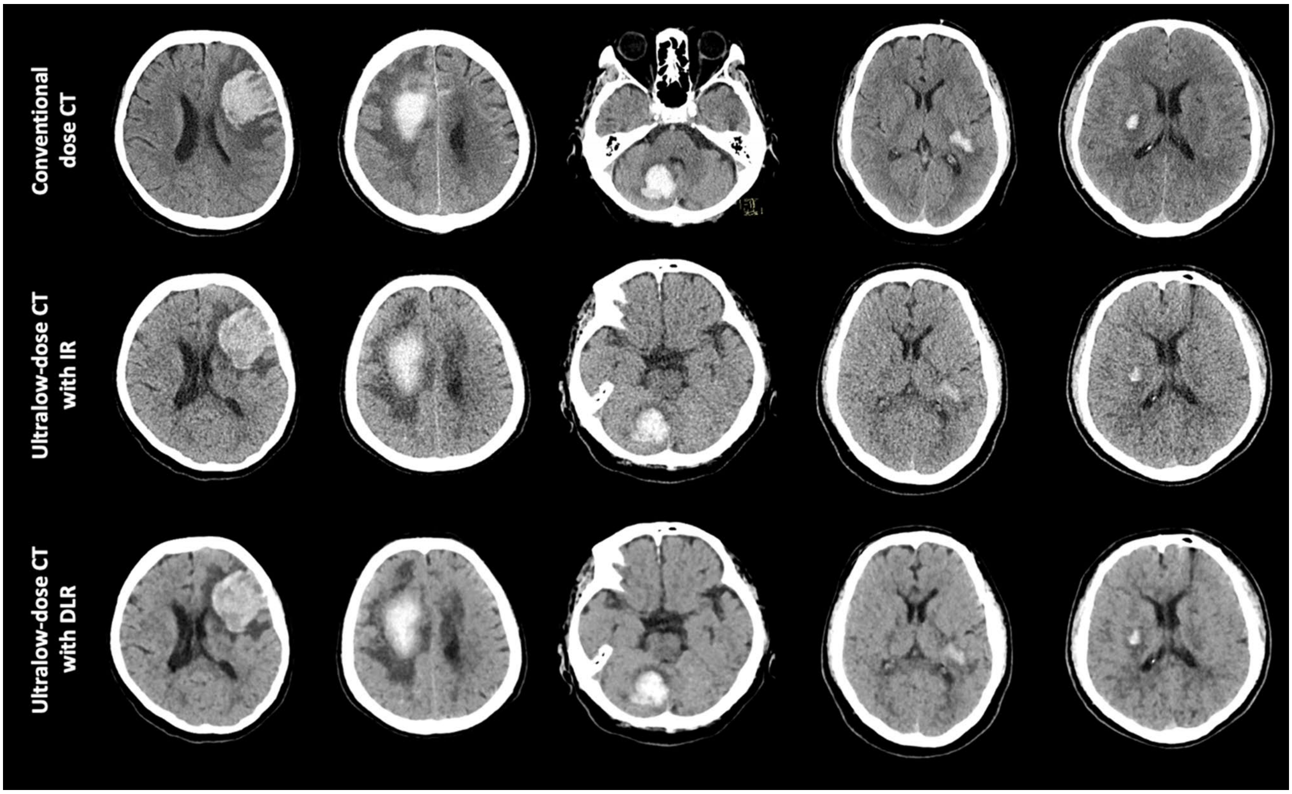

Fig. 4 Representative cases of intracranial hemorrhage with ultralow-dose protocols. The detection of intracranial hemorrhage was equivocal visualized for ultralow-dose CT protocols compared with conventional-dose CT. Perilesional edema was observed significantly better with ultralow-dose CT with deep learning reconstruction (DLR) than ultralow-dose CT with iterative reconstruction (IR). Furthermore, DLR improved image quality even in ultralow-dose CT protocol compared with IR. DLR: deep learning reconstruction, IR: iterative reconstruction

Ultralow-dose CT with DLR markedly reduces patient radiation exposure, in addition to providing higher image quality. The diagnostic performance for identifying intracranial hemorrhage was higher for ultralow-dose CT with DLR than for ultralow-dose CT with IR. Thus, ultralow-dose CT utilizing deep learning reconstruction (DLR) serves a critical role in both pre- and post-operative imaging by enabling accurate assessment of ventricular size and catheter positioning in ventriculoperitoneal shunting, as well as facilitating longitudinal surveillance of brain tumors, all while minimizing radiation exposure [28]. Finally, the application of ultralow-dose CT with DLR could minimize the risk of radiation exposure.

Our study has some limitations. First, the sample size was small, and the study design was retrospective, which may limit the generalizability of the findings. Second, we did not investigate the effect of a tube current of < 50 mA on the diagnostic performance of intracranial hemorrhage and image quality. The imaging parameters for ultralow-dose CT (tube voltage: 120 kVp and tube current: 50 mA) were based on a previous study that evaluated its use in detecting intracranial findings in patients with acute neurologic deficit [8]. Further validation is required to investigate a lower effective dose of < 0.21 mSv. Third, all results were limited to one scanner, and acquisition parameters may require adjustment for different CT scanner vendors. Fourth, we used the brain standard option for DLR, selecting it over the mild and strong strength settings. Additionally, we did not quantify hemorrhage size due to the dynamic progression of intracranial hemorrhage, including possible growth or expansion between initial and follow-up scans. Lastly, only thick-slice reconstructed images were analyzed in this study. Future research should explore the use of thinner slice reconstructions for improved detection of small-volume hemorrhages and assess the performance of ultralow-dose protocols across larger, prospective studies stratified by different types of intracranial hemorrhage.

Conclusions

Ultralow-dose CT with DLR is not inferior to conventional-dose CT in terms of image quality and diagnostic performance for the detection of intracranial hemorrhage, while achieving an approximate 87.7% reduction in radiation dose.

Abbrevations

DLR Deep learning reconstruction
CT Computed tomography

IR Iterative reconstruction
IQR Interquartile range
SNR Signal-to-noise ratio
SD Standard deviation
CSF Cerebrospinal fluid
CNR Contrast-to-noise ratio
GM Gray matter
WM White matter

Acknowledgements
Not applicable.

Author contributions
C. Otgonbaatar and J. W. Kim designed the research study. Otgonbaatar wrote the manuscript. J. K. Ryu and H. Shim provided help on the research. P. H. Jeon, S. H. Jeon, and S. J. Cha collected and investigated the data. H. Kim, S. M. Ko and J. W. Kim supervised the manuscript. J. W. Kim reviewed and edited the manuscript. All authors read and approved the final manuscript.

Funding
The authors state that this work has not received any funding.

Data availability
The datasets used and/or analysed during the current study are available from the corresponding author on reasonable request.

Declarations

Ethics approval and consent to participate
This retrospective study was approved by the Institutional Review Board of Wonju Severance Christian Hospital (IRB number: CR323171). The requirement for informed consent was waived because of the retrospective study design. The study was performed in accordance with relevant guidelines and regulations, including the Declaration of Helsinki.

Consent for publication
The requirement for informed consent was waived because of the retrospective study design.

Competing interests
The authors declare no competing interests.

Received: 3 February 2025 / Accepted: 20 November 2025
Published online: 24 November 2025

References

1. Dieckmeyer M, Sollmann N, Kupfer K, Löffler MT, Paprottka KJ, Kirschke JS, Baum T. Computed tomography of the head: A systematic review on acquisition and reconstruction techniques to reduce radiation dose. Clin Neuroradiol. 2023;33(3):591–610.
2. Law M, Ma WK, Lau D, Cheung K, Ip J, Yip L, Lam W. Cumulative effective dose and cancer risk for pediatric population in repetitive full spine follow-up imaging: how micro dose is the EOS microdose protocol? Eur J Radiol. 2018;101:87–91.
3. Ogino H, Fujimichi Y, Sasaki M, Hamada N, Iwasaki T, Yoshida K, Hattori T. Quantitative assessment of provability of radiation-related cancers considering unavoidable existence of unadjusted risk factors. J Radiol Prot. 2016;36(4):865–84.
4. Pearce MS, Salotti JA, Little MP, McHugh K, Lee C, Kim KP, Howe NL, Ronckers CM, Rajaraman P, Sir Craft AW, et al. Radiation exposure from CT scans in childhood and subsequent risk of leukaemia and brain tumours: a retrospective cohort study. Lancet. 2012;380(9840):499–505.
5. Mathews JD, Forsythe AV, Brady Z, Butler MW, Goergen SK, Byrnes GB, Giles GG, Wallace AB, Anderson PR, Guiver TA, et al. Cancer risk in 680,000 people exposed to computed tomography scans in childhood or adolescence: data linkage study of 11 million Australians. BMJ. 2013;346:f2360.
6. Smith AB, Dillon WP, Gould R, Wintermark M. Radiation Dose-Reduction strategies for neuroradiology CT protocols. Am J Neuroradiol. 2007;28(9):1628.
7. Nagayama Y, Oda S, Nakaura T, Tsuji A, Urata J, Furusawa M, Utsunomiya D, Funama Y, Kidoh M, Yamashita Y. Radiation dose reduction at pediatric CT: use of low tube voltage and iterative reconstruction. Radiographics. 2018;38(5):1421–40.
8. Fletcher JG, DeLone DR, Kotsenas AL, Campeau NG, Lehman VT, Yu L, Leng S, Holmes DR 3rd, Edwards PK, Johnson MP, et al. Evaluation of Lower-Dose spiral head CT for detection of intracranial findings causing neurologic deficits. AJNR Am J Neuroradiol. 2019;40(11):1855–63.
9. Alagic Z, Diaz Cardenas J, Halldorsson K, Grozman V, Wallgren S, Suzuki C, Helmenkamp J, Koskinen SK. Deep learning versus iterative image reconstruction algorithm for head CT in trauma. Emerg Radiol. 2022;29(2):339–52.
10. Sun J, Li H, Wang B, Li J, Li M, Zhou Z, Peng Y. Application of a deep learning image reconstruction (DLIR) algorithm in head CT imaging for children to improve image quality and lesion detection. BMC Med Imaging. 2021;21(1):108.
11. Kim I, Kang H, Yoon HJ, Chung BM, Shin NY. Deep learning-based image reconstruction for brain CT: improved image quality compared with adaptive statistical iterative reconstruction-Veo (ASIR-V). Neuroradiology. 2021;63(6):905–12.
12. Otgonbaatar C, Kim H, Jeon PH, Jeon SH, Cha SJ, Ryu JK, Jung WB, Shim H, Ko SM, Kim JW. A preliminary study of super-resolution deep learning reconstruction with cardiac option for evaluation of endovascular-treated intracranial aneurysms. Br J Radiol. 2024;97(1160):1492–500.
13. Otgonbaatar C, Ryu JK, Kim S, Seo JW, Shim H, Hwang DH. Improvement of depiction of the intracranial arteries on brain CT angiography using deep learning reconstruction. J Integr Neurosci. 2021;20(4):967–76.
14. Shrimpton PC, Hillier MC, Lewis MA, Dunn M. National survey of doses from CT in the UK: 2003. Br J Radiol. 2006;79(948):968–80.
15. Tan Z, Zhang L, Sun X, Yang M, Makamure J, Wu H, Wang J. Dual-Layer detector head CT to maintain image quality while reducing the radiation dose in pediatric patients. AJNR Am J Neuroradiol. 2023;44(10):1212–8.
16. Bodelle B, Klein E, Naguib NN, Bauer RW, Kerl JM, Al-Butmeh F, Wichmann JL, Ackermann H, Lehnert T, Vogl TJ, et al. Acute intracranial hemorrhage in CT: benefits of sinogram-affirmed iterative reconstruction techniques. AJNR Am J Neuroradiol. 2014;35(3):445–9.
17. Koo TK, Li MY. A guideline of selecting and reporting intraclass correlation coefficients for reliability research. J Chiropr Med. 2016;15(2):155–63.
18. Koetzier LR, Mastrodicasa D, Szczykutowicz TP, van der Werf NR, Wang AS, Sandfort V, van der Molen AJ, Fleischmann D, Willemink MJ. Deep learning image reconstruction for CT: technical principles and clinical prospects. Radiology. 2023;306(3):e221257.
19. Otgonbaatar C, Ryu J-K, Shin J, Woo JY, Seo JW, Shim H, Hwang DH. Improvement in image quality and visibility of coronary Arteries, Stents, and valve structures on CT angiography by deep learning reconstruction. Korean J Radiol. 2022;23(11):1044–54.
20. van Stiphout JA, Driessen J, Koetzier LR, Ruules LB, Willemink MJ, Heemskerk JWT, van der Molen AJ. The effect of deep learning reconstruction on abdominal CT densitometry and image quality: a systematic review and meta-analysis. Eur Radiol. 2022;32(5):2921–9.
21. Park C, Choo KS, Jung Y, Jeong HS, Hwang JY, Yun MS. CT iterative vs deep learning reconstruction: comparison of noise and sharpness. Eur Radiol. 2021;31(5):3156–64.
22. Lyoo Y, Choi YH, Lee SB, Lee S, Cho YJ, Shin SM, Phi JH, Kim SK, Cheon JE. Ultra-low-dose computed tomography with deep learning reconstruction for craniosynostosis at radiation doses comparable to skull radiographs: a pilot study. Pediatr Radiol. 2023;53(11):2260–8.
23. Nakai Y, Miyazaki O, Kitamura M, Imai R, Okamoto R, Tsutsumi Y, Miyasaka M, Ogiwara H, Miura H, Yamada K, et al. Evaluation of radiation dose reduction in head CT using the half-dose method. Jpn J Radiol. 2023;41(8):872–81.
24. Meulepas JM, Ronckers CM, Smets A, Nievelstein RAJ, Gradowska P, Lee C, Jahnen A, van Straten M, de Wit MY, Zonnenberg B, et al. Radiation exposure from pediatric CT scans and subsequent cancer risk in the Netherlands. J Natl Cancer Inst. 2019;111(3):256–63.
25. Lee KH, Lee S, Park JH, Lee SS, Kim HY, Lee WJ, Cha ES, Kim KP, Lee W, Lee JY, et al. Risk of hematologic malignant neoplasms from abdominopelvic computed tomographic radiation in patients who underwent appendectomy. JAMA Surg. 2021;156(4):343–51.
26. Feng ST, Law MW, Huang B, Ng S, Li ZP, Meng QF, Khong PL. Radiation dose and cancer risk from pediatric CT examinations on 64-slice CT: a Phantom study. Eur J Radiol. 2010;76(2):e19–23.

27. Löbrich M, Rief N, Kühne M, Heckmann M, Fleckenstein J, Rübe C, Uder M. In vivo formation and repair of DNA double-strand breaks after computed tomography examinations. Proc Natl Acad Sci U S A. 2005;102(25):8984–9.
28. Jeggo PA, Löbrich M. DNA double-strand breaks: their cellular and clinical impact? Oncogene. 2007;26(56):7717–9.
29. Sakane H, Ishida M, Shi L, Fukumoto W, Sakai C, Miyata Y, Ishida T, Akita T, Okada M, Awai K, et al. Biological effects of Low-Dose chest CT on chromosomal DNA. Radiology. 2020;295(2):439–45.
30. Frija G, Damilakis J, Paulo G, Loose R, Vano E. Cumulative effective dose from recurrent CT examinations in europe: proposal for clinical guidance based on an ESR EuroSafe imaging survey. Eur Radiol. 2021;31(8):5514–23.

Publisher's note